



ELSEVIER

Earth and Planetary Science Letters 206 (2003) 199–214

EPSL

[www.elsevier.com/locate/epsl](http://www.elsevier.com/locate/epsl)

# Paleomagnetic evidence from Cape Verde Islands basalts for fully reversed excursions in the Brunhes Chron

Mads Faurschou Knudsen<sup>a,\*</sup>, Niels Abrahamsen<sup>a</sup>, Peter Riisager<sup>b,c</sup>

<sup>a</sup> Department of Earth Sciences, University of Aarhus, Finlandsgade 6–8, 8200 Aarhus N, Denmark

<sup>b</sup> Department of Earth Sciences, University of California at Santa Cruz, 1156 High Street, Santa Cruz, CA 95064, USA

<sup>c</sup> Danish Lithosphere Centre, Øster Voldgade 10, 1350 København, Denmark

Received 1 July 2002; received in revised form 1 November 2002; accepted 3 November 2002

## Abstract

In this study we present paleomagnetic data from two lava sequences on Santo Antão, Cape Verde Islands: the Tarrafal and Agua Nova profiles from which 63 and 43 lava flows were sampled, respectively. Previous  $^{40}\text{Ar}/^{39}\text{Ar}$  ages have constrained the two profiles to the Brunhes Chron, which is in accordance with the normal polarity of the majority of the flows. Some individual lava flows as well as flow sequences with virtual geomagnetic poles deviating more than  $45^\circ$  from the geographic North Pole are interpreted to represent geomagnetic excursions. Based on interpretation of the directional data three excursions are recorded in the Tarrafal profile (T-I, T-II, and T-III) and four in the Agua Nova profile (AG-I, AG-II, AG-III, and AG-IV). Both  $^{40}\text{Ar}/^{39}\text{Ar}$  results and paleomagnetic directional data indicate that an excursion defined by eight flows in the Tarrafal profile (T-I) is the same as one recorded in six flows in the Agua Nova profile (AG-I). This excursion, which passes the reversal test with classification C, is the first geomagnetic excursion in the Brunhes Chron to pass the reversal test. The  $^{40}\text{Ar}/^{39}\text{Ar}$  ages suggest that this excursion could represent chryptochron C1n-1 (0.493–0.504 Ma), the only chryptochron or ‘tiny wiggle’ identified in the marine magnetic anomaly record for the Brunhes Chron. The remaining excursions may not yet be unambiguously correlated between the two profiles. Another excursion recorded by two flows in the top of the Tarrafal profile (T-III) also displays completely reversed polarity.

© 2002 Elsevier Science B.V. All rights reserved.

*Keywords:* magnetic excursions; geomagnetic polarity intervals; Brunhes; chryptochrons; Cape Verde

## 1. Introduction

The last geomagnetic polarity reversal took

place  $\sim 780$  ka ago [1,2], marking the beginning of the present period of normal polarity, i.e. the Brunhes Chron. The geomagnetic field, however, has not been dominated by an axial dipole throughout the entire Brunhes Chron as evidenced by several well-documented geomagnetic excursions [2], where the virtual geomagnetic pole (VGP) deviated more than  $45^\circ$  from the geographic pole. Records from North Atlantic sediments indicate the existence of as many as 14 ex-

\* Corresponding author. Tel.: +45-89424334;

Fax: +45-86101003.

E-mail addresses: [madfsk@geo.au.dk](mailto:madfsk@geo.au.dk) (M.F. Knudsen), [abraham@geo.au.dk](mailto:abraham@geo.au.dk) (N. Abrahamsen), [peter@es.ucsc.edu](mailto:peter@es.ucsc.edu) (P. Riisager).

cursions in the Brunhes [3], suggesting that the geodynamo may have spent up to 20% of the Brunhes in a weak non-dipole state [3,4]. There exists no compelling paleomagnetic or geomagnetic evidence indicating that this high frequency of excursions should be confined to the Brunhes and not occur in other magnetochrons. Evidence suggests no less than seven excursions in the reverse Matuyama Chron between 1.18 and 0.78 Ma [5]. Although ‘tiny wiggles’ originally were thought to arise from variations in paleointensity [6], some of the chryptochrons (or tiny wiggles) recorded in older marine magnetic anomalies most likely represent geomagnetic excursions too [7,8].

Doell and Cox [9] originally suggested that geomagnetic excursions represent ‘aborted reversals’, i.e. a geomagnetic polarity transition which never completed before returning to the original polarity state. This suggestion is supported by recent numerical dynamo models [10] in which excursions correspond to short periods when only the field outside the tangent cylinder of the core reverses polarity while the field inside the tangent cylinder remains unchanged. Similarly, considerations of magnetic inertia in the inner and outer core [11] have led to the suggestion that an excursion arises from a change in geomagnetic field polarity in the liquid outer core but not in the solid inner core before the original polarity re-establishes itself fully. Detailed paleomagnetic records of excursions provide indispensable constraints for geodynamic modeling and the understanding of the processes generating the Earth’s magnetic field [12].

The Geomagnetic Instability Timescale (GITS), which is adopted in the present paper, is a term proposed by Singer et al. [2] for registration of geomagnetic excursions in the magnetic polarity record. The most recent GITS is mainly based on studies of high resolution sediment records. Unfortunately, the reliability of magnetic directions inferred from sediments can be compromised by both sampling procedure and the remanence acquisition, being particularly vulnerable to smoothing when the geomagnetic field is weak and/or undergoes rapid changes [7,13,14]. Ideally, the presence of excursions should be confirmed or

complemented by information from lava flows [4]. Only five excursions in the Brunhes (out of 14) are presently believed to be documented by volcanic rocks: Laschamps (40–45 ka) [15], Blake (110–120 ka) [16,17], Jamaica (205–215 ka) [18], possibly Calabrian Ridge 2 (515–525 ka) [19], and Big Lost (560–580 ka) [2,16,20].

In this paper we present paleomagnetic data from a reconnaissance study of lava flow sequences on the island of Santo Antão, Cape Verde Islands. Samples were collected from two profiles, which are constrained to the Brunhes Chron by  $^{40}\text{Ar}/^{39}\text{Ar}$  ages [21]. Both profiles contain short sequences of lava flows recording excursions, some of which deviate 180° from the Brunhes normal-polarity pole.

## 2. Geological setting

The Cape Verde archipelago (Fig. 1a) is believed to be the result of slow eastward movement of the African lithosphere plate relative to a hotspot with two active centers, resulting in a horseshoe-shaped configuration of islands opening westwards [22,23]. The bulk of the igneous activity took place around 19–20 Ma ago [24,25]. The archipelago shows increasing erosion towards the east, indicating that the more westerly parts of the archipelago are youngest. The underlying oceanic crust has ages between ca. 122 and 140 Ma [26, 27], corresponding to Mesozoic marine anomalies M2–M16 (Fig. 1a). The hotspot area gives rise to a topographic dome some 500 km in diameter (Fig. 1a) rising more than 2 km above the oceanic floor, the so-called Cape Verde Rise [28], on which the islands are situated. Thickened crust composed of uplifted, deformed Jurassic oceanic crust, plutonic rocks and sediments forms the geological basement of the islands [23,27,29]. Hotspot volcanics on the islands consist of silica-undersaturated lavas different from MORB, such as nephelinite, basanite and ankaramite, derived from magma formed by a low degree of partial melting of mantle peridotite at considerable depth [24,28].

We present paleomagnetic data in this paper from the island of Santo Antão (Fig. 1b) which

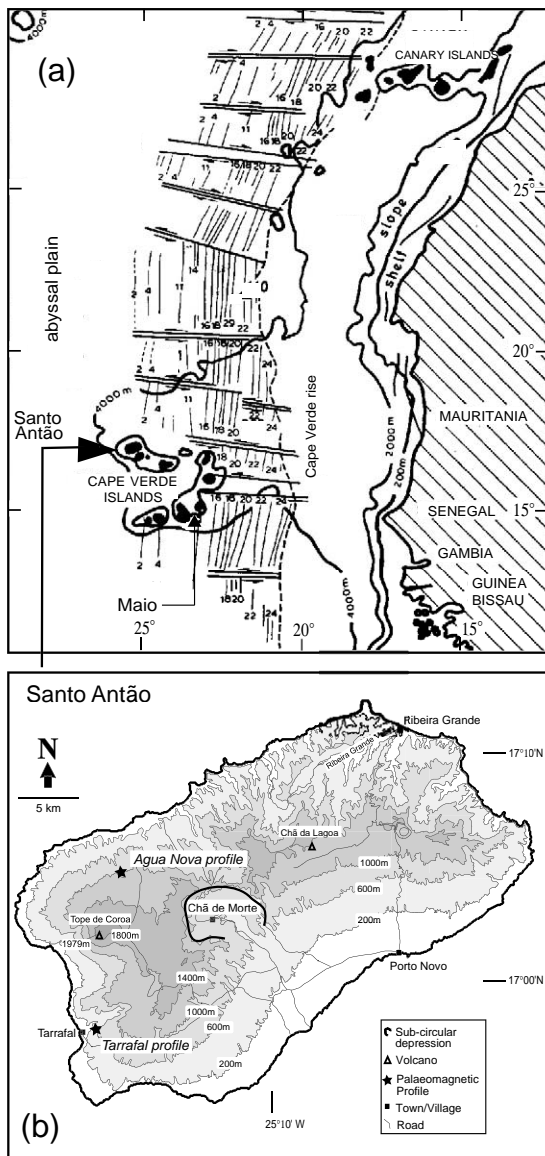


Fig. 1. (a) The Cape Verde Rise and regional magnetic marine anomalies, modified from Stillman et al. [27]. (b) The island of Santo Antão (map modified from Plesner et al. [47]) with the geographical locations of the Tarrafal (Lat.  $16^{\circ}57'00''\text{N}$ , Long.  $25^{\circ}18'20''\text{W}$ ) and Agua Nova (Lat.  $17^{\circ}3'50''\text{N}$ , Long.  $25^{\circ}17'25''\text{W}$ ) profiles.

covers an area of  $780 \text{ km}^2$  and has high topographic relief, with the summit of Tope de Coroa reaching an elevation of 1979 m above sea level. The island consists of lava sequences several hundred meters thick, which laterally cover large

areas. The recent  $^{40}\text{Ar}/^{39}\text{Ar}$  study by Plesner et al. [21] reveals ages between 0.09 and 7.57 Ma for the lavas on the island. The highest elevations correspond to the youngest ages, with Tope de Coroa having an age of  $0.17 \pm 0.02 \text{ Ma}$  [21], while the oldest exposures on Santo Antão are deeply weathered basalts located in the Chã de Morte Area ( $7.57 \pm 0.56 \text{ Ma}$ ) (Fig. 1b).

Few paleomagnetic studies have previously been undertaken on the Cape Verde Islands [30–33] and only Watkins et al. [30] and Knudsen and Abrahamsen [33] undertook such work on Santo Antão (Fig. 1b). Their data, though, stem from other areas, partly with complex stratigraphy, and cannot yet be correlated with the Tarrafal and Agua Nova profiles presented in this study.

### 2.1. Sampling

Paleomagnetic samples were collected along two major profiles separated by a horizontal distance of 15 km (Fig. 1b). Based on the field observations it is difficult to directly correlate the two profiles. However, similar isotope geochemistry in the upper and lower parts of the two profiles (P.M. Holm, personal communication), respectively, suggests tapping of the same magma sources and hence synchronous time of formation.

The superbly exposed Tarrafal profile is located in a steep-sided valley stretching inland from the Tarrafal village (Fig. 1b) and consists of approximately 100 lava flows with a simple stratigraphy. The profile covers a thickness of 500 m of near-horizontal flows, dipping  $2^{\circ}$  towards WNW on an original slope. Thin sequences of ankaramitic lava flows are found alternating with aphanitic lava flows and less than 10% pyroclastic material, mainly lapilli. The ankaramitic lava flows are typically 1–3 m thick and contain up to 40% olivine and clinopyroxene phenocrysts. The aphanitic flows may be up to 5 m thick. Towards the top of the profile, paleo-drainage channels filled by subsequent flows indicate that this part of the section encompasses significant geological time. At the Tarrafal profile, samples were collected from 63 individual lava flows evenly distributed among the approximately 100 flows.

The Agua Nova profile (Fig. 1b) is located in a

canyon in the NW part of the island and covers a vertical section of 200 m of flows, bedding on what we believe is an original slope of approximately  $10^\circ$  NW. The profile has an increasing frequency upwards of intervening pyroclastic layers of local origin. The lava flows are divided into a lower sequence of ankaramitic flows ( $\sim 30$  m and 10 flows), containing up to 60% olivine and clinopyroxene phenocrysts, and the major upper part of aphanitic or less commonly porphyritic flows ( $\sim 170$  m and 52 flows) with a tendency to be more vesicular than the ankaramitic flows. The flows in the lower parts of the profile are thicker and of a more varied texture than the upper flows, which tend to show a high degree of weathering. From the Agua Nova profile 43 of the altogether 62 flows were sampled.

In both profiles only one hand sample was collected from the individual lava flows, except for four flows in the Tarrafal profile (T213, T267, T268, and T274) where two samples were taken for proof of consistency in direction. Obviously, one hand sample from each lava flow is too little to form a foundation for solid conclusions, but due to a combination of extremely difficult field

conditions, where climbing was often necessary, and lack of time it was impossible to perform a more exhaustive collection. All samples were oriented by use of magnetic compass. Both profiles are tectonically undisturbed and no tilt correction of the paleomagnetic data is necessary.

### 3. Magnetic results

Rock magnetic experiments were carried out in order to study the magnetomineralogy of the studied samples. Measurements of the susceptibility as a function of temperature revealed titanomagnetite to be the dominant magnetic mineral, with a varying content of titanium. The varying titanomagnetite composition is illustrated in Fig. 2: Fig. 2a shows a reversible heating curve with one Curie temperature and possibly a Verwey transition, both indicating titanium-poor titanomagnetite ( $\sim$ TM0–TM5), and Fig. 2b shows a non-reversible heating curve with two distinct titanomagnetite phases, one being titanium-poor and the other titanium-rich with an approximate composition of TM70. The majority of the Tarr-

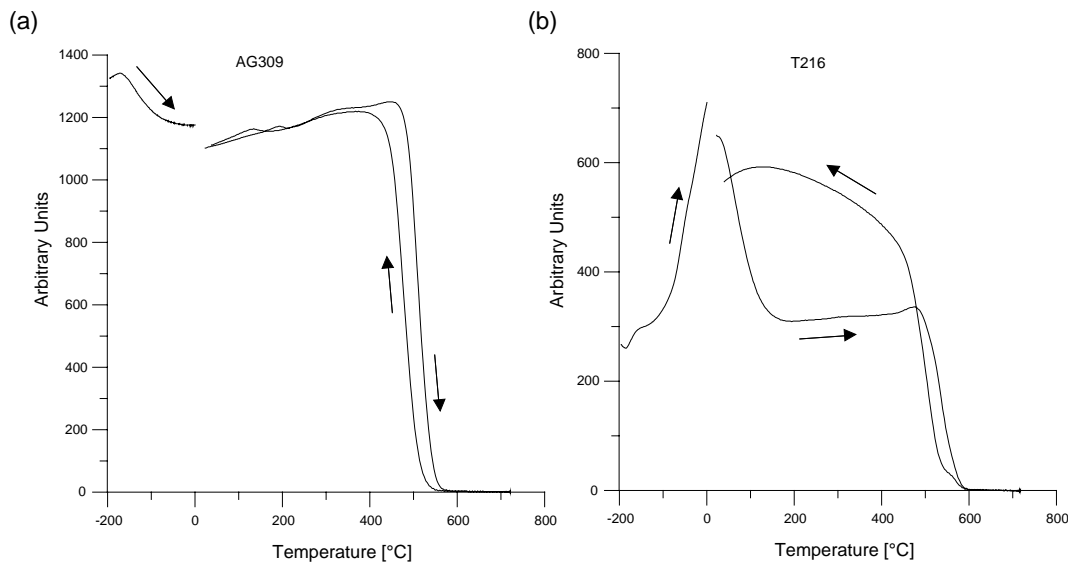


Fig. 2. Weak-field magnetic susceptibility as a function of temperature for samples (a) AG309 (Agua Nova) and (b) T216 (Tarrafal). The reversible heating curves along with a Verwey transition at  $-160^\circ\text{C}$  in (a) indicate the presence of single-phase titanium-poor titanomagnetite ( $\sim$ TM0–5), while the irreversible curves in (b) show two magnetic phases, i.e. titanium-rich titanomagnetite ( $\sim$ TM70) and close to pure magnetite ( $\sim$ TM0–5).

fal and Agua Nova flows display behavior in between those depicted in Fig. 2a,b, with no obvious difference between the profiles or between flows of normal and excursions polarity. We interpret these data to indicate varying degrees of high-temperature (deuteric) oxidation of the primary titanomagnetite. The magnetic domain states of the Tarrafal and Agua Nova samples are illustrated in a Day plot [34] (Fig. 3), with the pseudo-single-domain (PSD) boundary values of Dunlop [35] applied. In general the measured flows plot close to the single-domain (SD) region. Also shown on the plot are the theoretical linear mixing curves of Dunlop for mixtures of SD and multidomain (MD) magnetite grains [35], which seem to fit the data reasonably well.

Paleomagnetic experiments were also carried out in order to isolate the characteristic remanent magnetization (ChRM). All specimens were subjected to stepwise alternating field demagnetization. The ChRM components were in almost all cases easily defined by principal component anal-

ysis [36], as the Zijderveld diagrams display stable single-component magnetizations with typically little or no evidence of secondary magnetization. Only three samples from each profile were omitted due to poor sample behavior probably caused by large magnetic viscosity. Fig. 4 shows two typical Zijderveld diagrams for specimens from each of the Tarrafal and Agua Nova profiles. ChRM directions proved consistent for the flows where two hand samples were collected (T213, T267, T268, and T274). A quantitative measure of the precision is expressed through the low average maximum angular deviation of typically 1°–2° (see Table 1). ChRM directions for all flows in the two profiles are presented in Fig. 5 and Table 1. The directions presented for each lava flow in Table 1 stem from only one sample and where two hand samples were collected the sample with the best-defined ChRM is presented.

### 3.1. The Tarrafal profile

Fig. 5a shows the ChRM declination and inclination of the studied flows in the stratigraphic sequence.  $^{40}\text{Ar}/^{39}\text{Ar}$  whole-rock and ground-mass dates from this section confine the profile to the Brunhes Chron. Flow T213 (ground-mass age) yields a plateau age of  $0.54 \pm 0.09$  Ma ( $\pm 1\sigma$ ), defined by three steps and 44.9% release of the total  $^{39}\text{Ar}$ . The  $^{40}\text{Ar}/^{36}\text{Ar}$  intercept of  $295 \pm 13$  is in good accordance with the atmospheric ratio, 295.5 [2]. For flow T267 (whole-rock age) the isochron age of  $0.38 \pm 0.05$  Ma ( $\pm 1\sigma$ ) is believed to reflect the true age of the flow (67.5% total release of  $^{39}\text{Ar}$ ). An  $^{40}\text{Ar}/^{36}\text{Ar}$  intercept of  $299 \pm 2$  indicates the presence of excess argon, which explains the slightly higher plateau age ( $0.43 \pm 0.01$  Ma) [21].

Defining excursions as VGPs deviating more than 45° from the geographic pole, three sequences of flows, labeled T-I, T-II, and T-III, display excursions behavior (Fig. 5a). The stereogram in Fig. 6a shows the ChRM direction of all the sampled flows in the profile, while Table 2 lists the mean paleomagnetic directions and the associated statistical parameters along with the paleomagnetic pole for the normal-polarity flows and VGPs for the different sequences of excursions

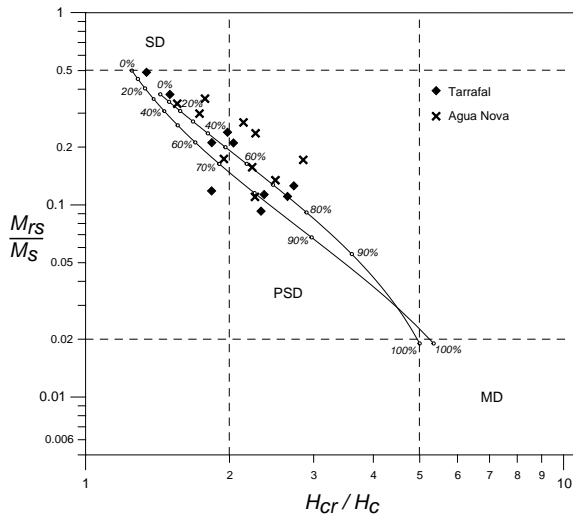


Fig. 3. Day plot [34] for samples from the Tarrafal and Agua Nova profiles, with the magnetite PSD-range boundary values of Dunlop [35]. The lines shown in the Day plot are theoretical linear mixing curves for mixtures of SD and MD-pure magnetite grains [35] with two different sets of SD and MD end-members (numbers denote percentage MD grains). According to Dunlop's linear mixing theory for SD and MD magnetite grains, the Tarrafal and Agua Nova samples range from close to pure SD domain to 20–30%SD+70–80%MD.

Table 1

The ChRM declination and inclination are listed sequentially from the uppermost flow and downwards through the two profiles along with the NRM intensity, maximum angular deviation, alternating field demagnetization steps used in the PCA, and susceptibility

Tarrafal	Dec (°)	Inc (°)	Int (A/m)	MAD (°)	PCA (mT)	$\chi$ [10 <sup>-3</sup> SI]
T325	9.0	19.8	3.63	0.9	10–100	45
T324	359.4	10.3	3.82	1.2	5–100	47
T323	6.3	24.2	5.37	1.6	20–100	1.2
T322	8.6	18.3	2.91	1.1	5–100	51
T321	348.9	22.2	2.75	1.6	0–100	65
T320	347.8	28.4	3.42	1.6	5–100	52
T319	353.4	10.2	4.38	2.1	0–100	57
T274	332.4	31.1	26.7	1.0	10–100	57
T272	0.6	38.4	19.4	1.2	5–100	29
T271	18.4	28.9	7.32	1.2	10–100	28
T268	2.7	29.5	6.22	0.8	0–100	25
T267	345.3	38.8	4.37	2.3	10–100	38
T265	21.3	31.0	3.99	1.5	10–100	95
T264	183.6	-15.3	2.29	0.9	5–100	90
T263	192.6	-3.3	5.54	0.9	5–100	39
T262	22.4	8.2	2.24	1.3	7.5–100	35
T261	4.6	-2.2	3.79	2.7	10–100	59
T260	6.9	7.6	2.77	1.6	10–100	26
T257	346.2	12.1	1.54	1.0	10–100	42
T255	6.1	16.9	2.35	1.0	10–100	15
T254	0.6	8.0	2.88	3.5	0–100	24
T253	356.1	29.9	3.53	1.7	5–100	23
T252	1.3	31.4	5.53	1.3	5–100	20
T251	357.1	32.2	5.46	2.1	5–100	19
T250	4.4	21.8	8.71	1.0	10–100	34
T249	325.2	21.7	6.40	2.1	10–100	38
T248	350.7	7.9	3.74	0.9	5–100	33
T246	349.6	48.1	3.97	1.9	7.5–100	21
T245	356.5	54.2	5.91	1.2	20–100	33
T244	354.4	57.1	5.18	1.9	7.5–100	21
T243	0.0	33.4	4.32	2.7	7.5–100	41
T241	26.8	5.1	3.92	1.5	5–100	30
T240	33.9	1.9	1.72	0.7	5–100	23
T239	45.8	-21.9	4.53	1.6	0–100	41
T238	354.9	26.9	3.88	5.1	10–80	29
T237	359.8	30.6	3.75	1.3	5–100	47
T236	355.9	29.2	5.22	1.4	10–100	34
T235	355.3	33.4	2.59	1.4	2.5–100	18
T234	14.7	32.1	4.80	0.9	5–100	31
T233	339.7	7.3	7.14	2.7	30–100	66
T232	5.5	31.1	5.80	1.2	10–100	52
T229	1.4	34.1	0.62	1.1	2.5–15	55
T230	173.5	-28.0	0.91	2.3	2.5–100	37
T227	207.9	-17.7	1.94	2.0	10–100	38
T225	184.8	-33.4	2.41	2.1	15–100	28
T224	172.4	-32.2	1.46	1.9	20–100	31
T223	169.7	-30.5	1.37	1.4	5–100	27
T220	184.5	-9.7	1.38	0.9	7.5–100	34
T218	191.8	-49.6	7.41	1.6	5–100	33
T216	178.7	-20.1	3.24	0.8	5–100	21
T215	342.0	42.1	7.19	1.4	10–60	64
T213	358.7	20.9	6.53	0.9	2.5–100	50

Table 1 (Continued).

Agua Nova	Dec (°)	Inc (°)	Int (A/m)	MAD (°)	PCA (mT) (mT)	$\chi$ [10 <sup>-3</sup> SI]
AG277	339.0	32.5	9.67	2.1	0–100	32
AG278	3.0	22.5	7.69	0.8	0–100	17
AG279	355.0	27.0	6.78	1.1	10–100	36
AG282	358.5	25.5	28.3	0.7	0–100	51
AG283	4.4	14.5	24.4	2.1	10–100	59
AG284	2.2	27.4	7.47	1.3	5–100	14
AG285	352.8	46.4	4.24	2.1	20–100	54
AG286	14.1	52.8	10.2	1.1	0–100	62
AG287	340.8	46.7	4.08	2.0	5–100	
AG318	11.8	42.9	4.14	2.4	0–100	56
AG317	37.6	47.3	2.03	1.8	0–100	1.9
AG315	169.1	32.9	4.73	1.5	5–100	38
AG314	22.0	36.5	5.59	0.9	10–100	57
AG313	10.9	6.2	8.34	2.1	0–100	54
AG311	189.1	–20.0	4.20	1.7	0–100	44
AG309	253.7	50.4	7.65	1.7	10–100	50
AG308	358.6	20.9	7.36	2.1	0–100	11
AG307	3.1	12.0	7.25	1.2	0–100	36
AG305	347.6	20.5	4.22	2.2	0–100	41
AG304	4.9	30.1	7.20	0.6	5–100	55
AG303	348.0	35.1	4.58	0.8	0–100	38
AG301	9.2	35.4	10.3	1.6	5–100	43
AG298	350.0	14.6	4.88	1.5	5–100	75
AG296	159.5	–4.0	2.47	3.3	10–100	40
AG294	323.7	58.0	8.59	1.2	0–100	50
AG293	164.1	–21.5	5.15	0.9	10–100	68
AG292	166.7	–9.3	4.16	0.9	10–100	66
AG291	141.5	–12.0	5.60	2.8	10–100	34
AG290	163.9	–43.8	4.76	1.0	5–100	15
AG289	173.6	–8.3	10.4	0.7	10–100	34
AG288	168.5	–2.9	6.13	1.3	5–100	14

Note that data presented for each flow stem from only one sample and where two hand samples were collected (T213, T267, T268, and T274) the sample with the best-defined ChRM is presented. The vertical thickness of the two profiles is  $\sim 500$  m (Tarrafal) and  $\sim 200$  m (Agua Nova), respectively.

flows. The reversal test of McFadden and Merrill [37] was performed for the mean direction of all normal-polarity flows compared to the mean direction of excursion T-I, containing eight flows. The reversal test was positive with classification C (angle between the two means = 3.8°), i.e. the antipode of the T-I mean direction is not distinguishable from the mean of the normal-polarity flows at the 95% confidence level.

### 3.2. The Agua Nova profile

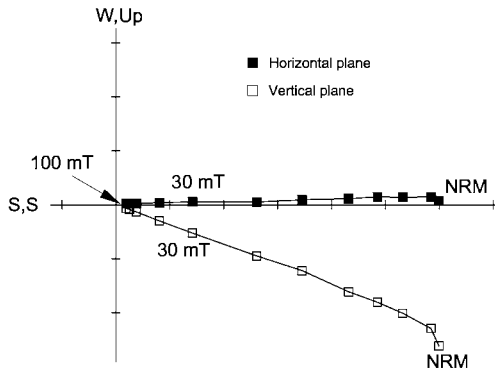
The ChRM declination and inclination of the Agua Nova flows are shown in Fig. 5b along with

the position of the dated flow (AG298). The AG298 (ground-mass age) yields a plateau age of  $0.52 \pm 0.01$  Ma ( $\pm 1\sigma$ ) based on seven steps and 95.2% of the total <sup>39</sup>Ar released [21]. An <sup>40</sup>Ar/<sup>36</sup>Ar intercept of  $292 \pm 3$  indicates that excess argon should not present a problem. The estimated isochron age agrees well with the plateau age ( $0.56 \pm 0.02$  Ma) [21].

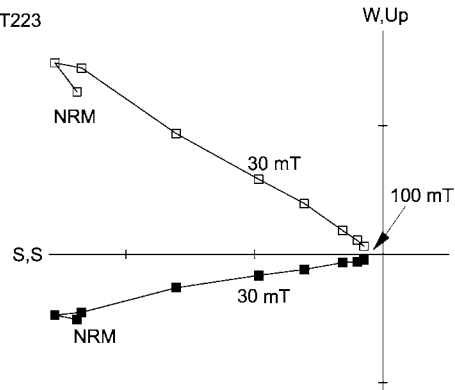
Altogether four excursions are found in the profile, labeled AG-I, AG-II, AG-III, and AG-IV (Fig. 5b). The stereogram in Fig. 6b displays the ChRM directions of the flows in the Agua Nova profile, while the relevant statistical parameters along with the paleomagnetic pole for the

## (a) Tarrafal profile

T213

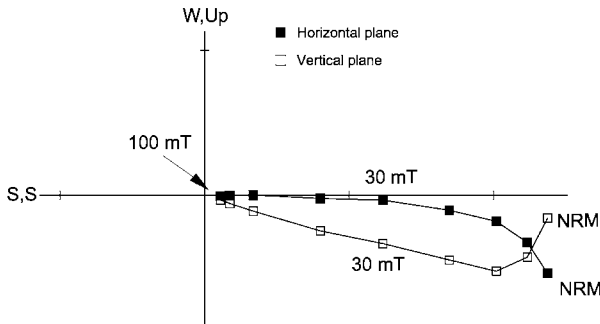


T223



## (b) Agua Nova profile

AG283



AG288

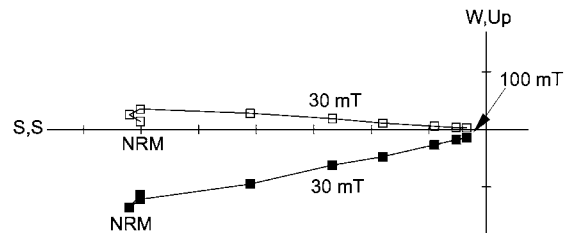


Fig. 4. Typical Zijderveld diagrams of alternating field demagnetization of (a) two Tarrafal flows and (b) two Agua Nova flows. Diagrams T223 and AG288 represent excursions T-I and AG-I in the Tarrafal and Agua Nova profiles, respectively.

normal-polarity flows and VGPs for excursions T-I and AG-I, respectively, are shown in Table 2. The mean directions of the AG-I excursion (six flows) and the normal-polarity flows fail to pass the reversal test (angle between the two means =  $21.9^\circ$ ) according to the criteria of McFadden and Merrill [37], and are thus distinct at the 95% level of confidence.

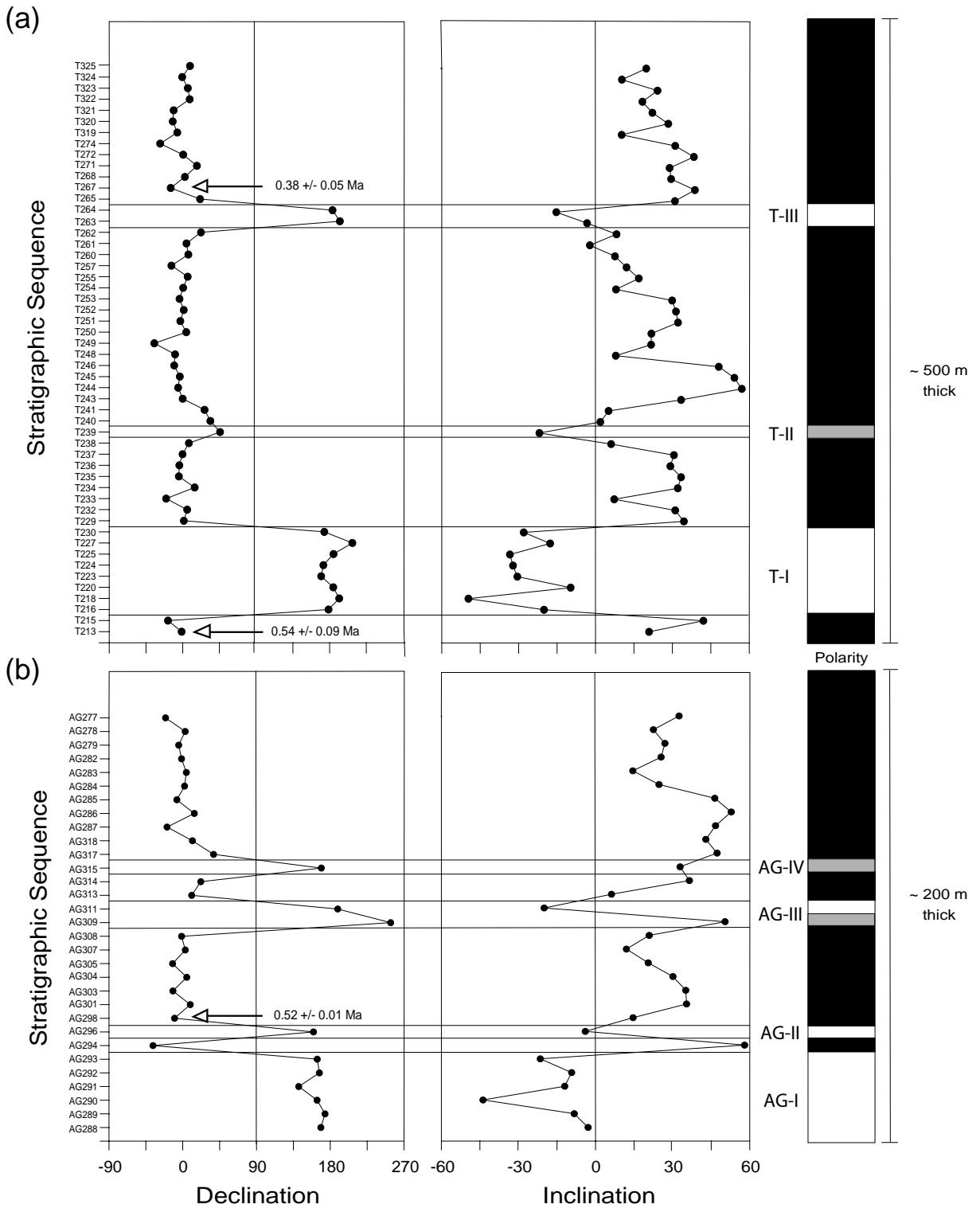
### 3.3. Paleomagnetic poles

VGPs for all normal-polarity flows in the Tar-

rafal and Agua Nova profiles are shown in Fig. 7a, while Fig. 7b shows the VGPs for reversed-polarity flows along with poles of intermediate direction. The two paleomagnetic poles derived from the normal-polarity flows in both profiles (Fig. 7c) are statistically indistinguishable (95% level of confidence) from the geographical North Pole. The VGP angular dispersion (VGP cut-off angle =  $45^\circ$ ) of the normal-polarity flows in the Tarrafal and Agua Nova profiles is  $S_{63} = 16.0^\circ$  ( $+2.89/-2.13$ ) and  $S_{63} = 17.5^\circ$  ( $+4.85/-3.13$ ), respectively, which is slightly above the predicted

Fig. 5. The ChRM declination and inclination of the flows in the stratigraphic sequence for (a) the Tarrafal profile ( $\sim 500$  m) and (b) the Agua Nova profile ( $\sim 200$  m). The polarity of the profiles and the labeled excursions are shown to the right. The  $^{40}\text{Ar}/^{39}\text{Ar}$  ages [21] of the dated flows (TT213, T267, and AG298) are also given (uncertainties on the presented ages are  $\pm 1\sigma$ ).





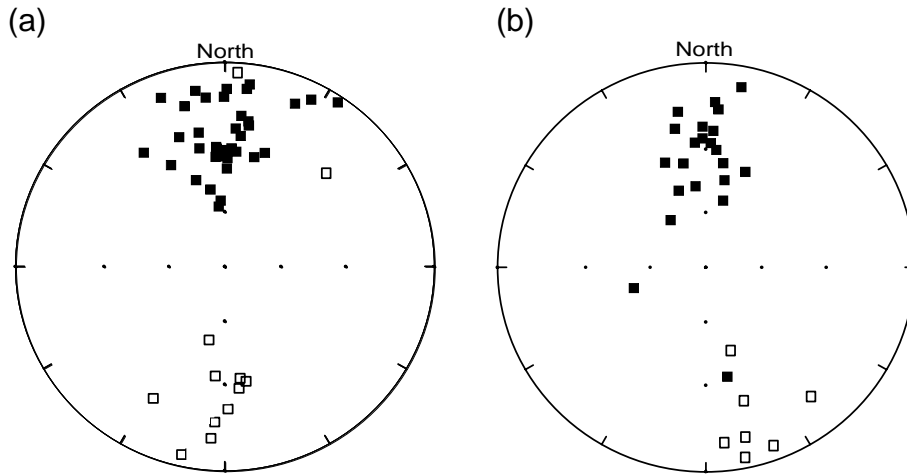


Fig. 6. Stereograms showing the ChRM direction of the flows in (a) the Tarrafal profile and (b) the Agua Nova profile.

value of approximately  $12.5^\circ$  for this latitude [38]. The paleomagnetic poles derived from the mean direction of excursions T-I (Tarrafal) and AG-I (Agua Nova) are shown in Fig. 7d along with the VGPs derived from the other excursions in the two profiles (T-II, T-III and AG-II, AG-III, AG-IV). Note that the paleomagnetic pole for excursion T-I is statistically indistinguishable from the geographical South Pole, whereas the pole for excursion AG-I plots slightly off the geographical pole (see Table 2). The two paleomagnetic poles deviating more than  $45^\circ$  from both geographical poles plot in or close to the preferred

VGP transition path, suggested by several authors [39–42].

## 4. Discussion

### 4.1. Correlation to the GITS

Before attempts are made to correlate the excursions observed in this study to the global GITS compilation of Singer et al. [2] (Fig. 8), it should be emphasized that the GITS presently continues to develop and undergo refinements [43]. One of

Table 2

For both profiles are listed the number of normal-polarity flows and flows in excursion sequences along with the mean declination and inclination and the associated  $\alpha_{95}$ ,  $\kappa$ , and  $S_{63}$

Profile	Samples	$N$	$D_m$ ( $^\circ$ )	$I_m$ ( $^\circ$ )	$\alpha_{95}$ ( $^\circ$ )	$\kappa$	$S_{63}$ ( $^\circ$ )	Plat ( $^\circ$ )	Plong ( $^\circ$ )	dp	dm
Tarrafal	Normal	41	0.0	25.4	5.2	19.2	16.0	86.4	154.0	3.0	5.6
Tarrafal	T-I	8	182.8	-28.2	11.4	24.5	14.4	86.7	100.1	6.8	12.5
Tarrafal	T-II (T239)	1	45.8	-21.9	-	-	-	-36.6	272.9	-	-
Tarrafal	T-III	2	188.2	-9.3	-	-	-	75.3	121.0	-	-
Agua Nova	Normal	21	0.1	31.9	7.5	18.9	17.5	89.7	352.4	4.7	8.4
Agua Nova	AG-I	6	163.1	-16.4	15.4	19.8	14.1	71.4	218.4	8.2	15.9
Agua Nova	AG-II (AG296)	1	159.5	-4.0	-	-	-	64.9	209.5	-	-
Agua Nova	AG-III (AG311)	1	189.1	-20.0	-	-	-	78.9	99.9	-	-
Agua Nova	AG-III (AG309)	1	253.7	50.4	-	-	-	-4.5	278.5	-	-
Agua Nova	AG-IV (AG315)	1	169.1	32.9	-	-	-	-53.5	351.6	-	-

Also listed are the coordinates and uncertainties of the corresponding paleomagnetic poles and VGPs.

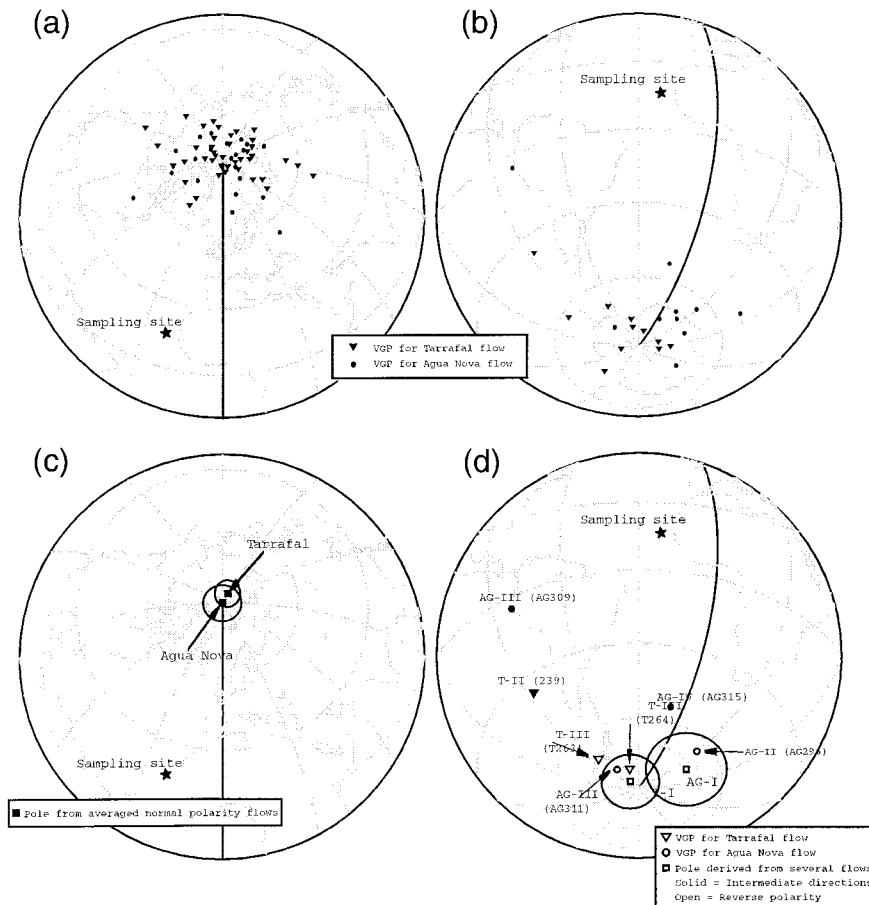


Fig. 7. VGPs for (a) all normal-polarity flows and (b) all reverse-polarity flows and flows with intermediate directions. (c) Paleomagnetic poles for all normal-polarity flows from the Tarrafal and Agua Nova profiles, and (d) excursions T-I and AG-I along with VGPs for the other excursions in the two profiles (T-II, T-III and AG-II, AG-III, AG-IV).

the uncertainties related to the GITS compilation stems from the uncertainties of absolute ages, which complicates the correlation of excursions recorded at different geographical localities. This has most recently been illustrated by observations of Kent et al. [44] suggesting that Mono Lake and Laschamp, both of which are included in the GITS [2], in fact represent the same excursion. Furthermore, only five of the postulated 14 Brunhes excursions have been observed in igneous rocks, which some authors consider a necessary criterion for excursions to be proven [4]. The ages of the excursions in the Tarrafal and Agua Nova profiles are not precisely defined, since the

$^{40}\text{Ar}/^{39}\text{Ar}$  ages only bracket the flows defining the excursions and not directly date the excursions themselves. Furthermore, the relatively large uncertainty on the ages of the dated flows excludes the possibility of uniquely correlating the Tarrafal and Agua Nova excursions to the GITS.

The lowermost dating in the Tarrafal profile indicates T-I to be younger than  $540 \pm 90$  ka, whereas the dating in the Agua Nova profile indicates AG-I to be older than  $520 \pm 10$  ka (Fig. 8). If we assume that T-I and AG-I recorded the same excursion, the age of this excursion would then be defined as older than  $520 \pm 10$  ka ( $\pm 1\sigma$ ) and younger than  $540 \pm 90$  ka ( $\pm 1\sigma$ ), which im-

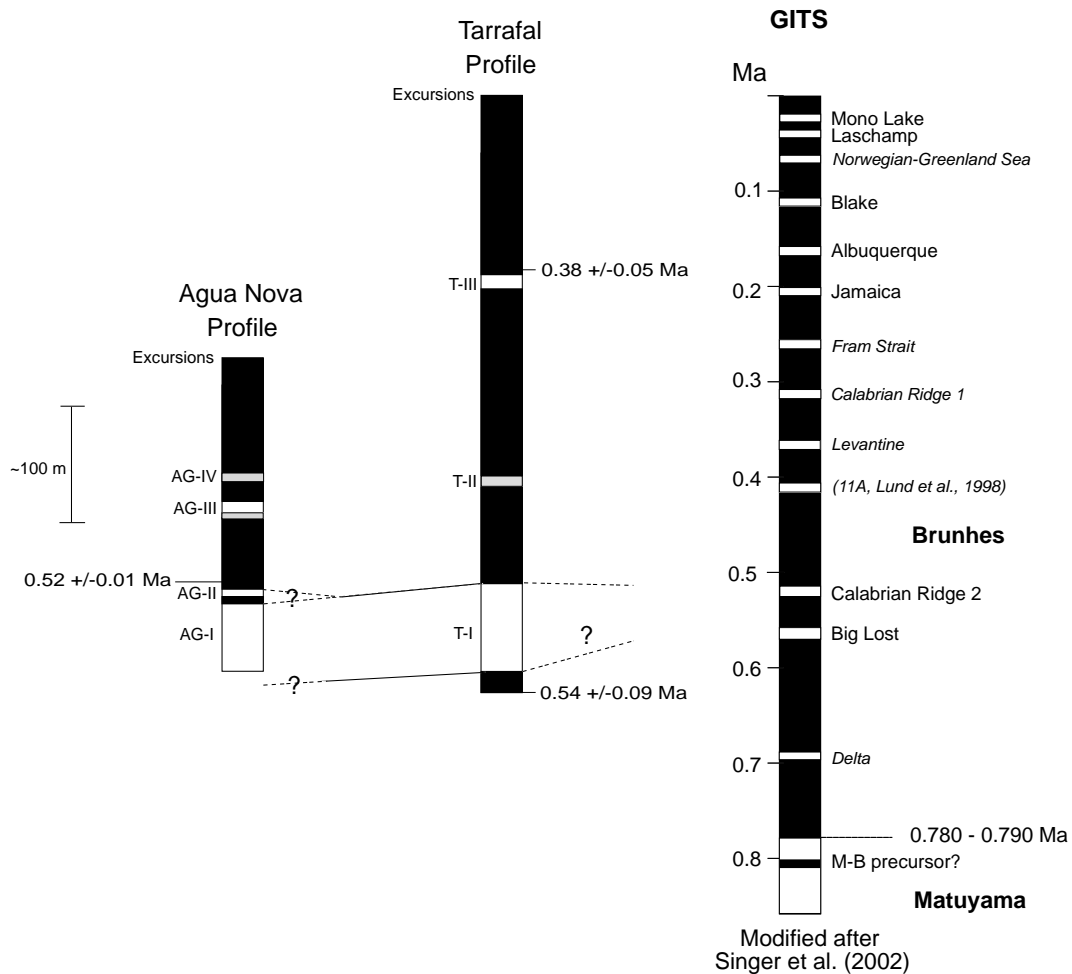


Fig. 8. Correlation between the Tarrafal and Agua Nova profiles and to the right their relation to the Geomagnetic Instability Time Scale [2] (proposed events which require further verification are labeled with italic letters). The correlation is constrained by the  $^{40}\text{Ar}/^{39}\text{Ar}$  ages [21] of the dated flows. Black corresponds to normal polarity and white to reverse polarity, whereas gray in the polarity scales for Tarrafal and Agua Nova indicates flows of intermediate direction.

plies the excursion could have occurred anywhere in the interval 500–720 ka (500 ka = 520 ka  $-2\sigma$  and 720 ka = 540 ka  $+2\sigma$ ). Consequently, the T-I and AG-I excursions may correspond to either the Calabrian Ridge 2, Big Lost or Delta excursions, since they all have an age within the interval 500–720 ka. The fact that the Calabrian Ridge 2 is observed to be nearly reversed in Mediterranean sediments [43] does make a correlation to this excursion more appealing.

We cannot exclude the possibility that T-I and AG-I correspond to two different excursions, but

only note that in addition to synchronous ages both excursions record several flows of fully reversed polarity, which has not been observed in other Brunhes excursions yet. It should be mentioned that even though their mean directions are statistically distinguishable (angle between the two means =  $22.1^\circ$ ), a reversal test comparing the combined mean direction of T-I and AG-I to the mean direction of all normal-polarity flows is positive with classification C. Only one ‘tiny wiggle’ or chryptochron is identified in the Brunhes Chron, i.e. C1n-1, which is estimated to span

the time interval 0.493–0.504 Ma [1]. Given that excursions T-I and AG-I have fully reversed directions and possibly a longer duration than the other excursions observed in our profiles, it could possibly represent the almost synchronous C1n-1 chryptochron, since no other fully reversed excursion have been observed in the Brunhes.

Due to the before-mentioned limited age control it is not possible to uniquely correlate the remaining excursions between the two profiles or to the GITS either. Excursion T-III in the Tarrafal profile is found right below a flow with an age of  $0.38 \pm 0.05$  Ma ( $\pm 1\sigma$ ), indicating that the excursion is older than 280 ka ( $280 \text{ ka} = 380 \text{ ka} - 2\sigma$ ). The only constraint given on the maximum age of T-III stems from the dating in the bottom of the profile ( $540 \pm 90$  ka), which provides a maximum-age constraint of 720 ka ( $720 \text{ ka} = 540 \text{ ka} + 2\sigma$ ). Consequently, excursion T-III may correspond to any excursion from the Calabrian Ridge 1 (315–325 ka, [43,45]) to the Delta excursion [46], but we favor a correlation to excursion 11A (age  $\sim 420$  ka) in the study of Lund et al. [3] which nearly completes a full reversal.

#### 4.2. Short-period geomagnetic polarity intervals in the Brunhes Chron

The most important feature of the excursions recorded in the Cape Verde volcanics is that the VGPs for some excursions deviate  $\sim 180^\circ$  from the geographic North Pole. Although excursions T-I and AG-I are the first Brunhes-aged excursions to pass the reversal test, they resemble older short-period geomagnetic excursions observed as ‘tiny wiggles’ or chryptochrons in the marine magnetic anomaly record [7,8]. Roberts and Lewin-Harris [7] show that some of the ‘tiny wiggles’ within Chron C5n.2n represent polarity intervals during which the field completed a full reversal and the associated intensity variation resembled the characteristics of a true polarity interval. Roberts and Lewin-Harris [7] further claim that statistical analyses of reversal time series predict the existence of polarity intervals that are shorter in duration than the minimum 30 ka intervals reported in the polarity time scales [1].

The paleomagnetic manifestations for geomag-

netic excursions and short-period polarity intervals appear distinct in terms of variation in field direction, intensity, and global extent during the magnetic event. This distinction possibly reflects a phenomenological difference between geomagnetic excursions and short polarity intervals, i.e. while geomagnetic excursions could reflect periods with high non-dipole to dipole field ratios, where the dipole generator is for some reason less efficient, the full short-period polarity reversal is characterized by a  $180^\circ$  change of the axial dipole. How the phenomenological difference is related to any difference in geomagnetic origin between geomagnetic excursions and short-period polarity intervals remains unclear. A geomagnetic excursion not reaching a full reversal is suggested to arise from polarity transitions in the outer core [11] or outside the ‘tangent cylinder’ [10] too short-lived to trigger a polarity transition in the inner core or inside the ‘tangent cylinder’. The full polarity reversal is believed to arise from field reversal in both the outer and inner core or alternatively both inside and outside the ‘tangent cylinder’ [7].

A short-period polarity interval characterized by fully reversed polarity would cause a global reversal of the geomagnetic field observable throughout the Earth. This means that observations from different locations of rocks with fully reversed polarity is required before an excursion can be classified as a polarity interval. The present study underlines the possible existence of short-period geomagnetic polarity intervals, but it is obviously premature to claim their presence in the Brunhes Chron from this study alone.

## 5. Conclusions

The Tarrafal and Agua Nova flows are largely constrained to the Brunhes Chron by  $^{40}\text{Ar}/^{39}\text{Ar}$  ages, which is in agreement with the majority of lava flows in both profiles possessing normal polarity. Our paleomagnetic reconnaissance study found three excursions in the Tarrafal profile and four in the Agua Nova profile. The eight-flow excursion T-I in the Tarrafal profile passes the reversal test (classification C) whereas the six-flow excursion AG-I in the Agua Nova profile

with the same age fails the reversal test. However, if the mean direction of excursions T-I and AG-I is compared to the mean direction of all normal-polarity flows from both profiles, the reversal test is positive with classification C. Since the data presented only rely on one sample from each lava flow (except for flows T213, T267, T268, and T274) and since, furthermore, no  $^{40}\text{Ar}/^{39}\text{Ar}$  ages exist for the exact flows defining the excursions, an unambiguous correlation to the GITS is not possible. We emphasize the importance of future detailed paleomagnetic studies of the Tarrafal and Agua Nova profiles in order to support the data and preliminary conclusions presented in this paper.

However, the study of the directional data from the Tarrafal and Agua Nova profiles does present some important and novel information on excursions in the Brunhes, since three flow sections with fully reversed polarity (T-I, AG-I, and T-III) are recorded in the two profiles. These are the first observations of excursions in volcanic rocks from the Brunhes, in which the magnetic-field polarity was fully reversed. Excursions T-I (Tarrafal profile) and AG-I (Agua Nova profile) most likely represent the same excursion, which we suggest corresponds to the only chrytochron observed in the Brunhes, i.e. chrytochron C1n-1 found in the 0.493–0.504 Ma interval in the marine magnetic anomaly record. The third flow section characterized by fully reversed polarity, denoted excursion T-III, consists of two flows located in the top of the Tarrafal profile.

### Acknowledgements

We thank the Danish National Science Foundation for financial support and our colleagues in the Danish Working Group on the Geology of the Cape Verde Islands for collaboration and help during field work. We further appreciate the collaboration and free laboratory facilities offered by Dr. Marek Lewandowski, Polish Academy of Sciences, Warsaw, Poland and Dr. Xixi Zhao, University of California, Santa Cruz, CA, USA. Valuable comments offered by Janna Riisager and Christopher Pluhar greatly improved the

early versions of this manuscript. We are grateful for the useful suggestions provided by the two reviewers, Dr. B. Singer and Dr. C. Johnson. [RV]

### References

- [1] S. Cande, D.V. Kent, Revised calibration of the geomagnetic polarity timescale for the Late Cretaceous and Cenozoic, *J. Geophys. Res.* 100 (1995) 6093–6095.
- [2] S. Singer, M.K. Relle, K.A. Hoffman, A. Battle, C. Laj, H. Guillou, J.C. Carracedo,  $^{40}\text{Ar}/^{39}\text{Ar}$  ages from transitionally magnetized lavas on La Palma, Canary Islands, and the geomagnetic instability timescale, *J. Geophys. Res.*, in press.
- [3] S.P. Lund, B. Acton, B. Clement, M. Hastedt, M. Okada, T. Williams, OPD Leg 172 Scientific Party, Geomagnetic field excursions occurred often during the last million years, in: *EOS Trans. AGU* 79, Spring Meet. Suppl. (1998) F178–F180.
- [4] R.T. Merrill, P.L. McFadden, Geomagnetic field stability: Reversal events and excursions, *Earth Planet. Sci. Lett.* 121 (1994) 57–59.
- [5] B. Singer, K.A. Hoffman, A. Chauvin, R.S. Coe, M.S. Pringle, Dating transitionally magnetised lavas of the Matuyama Chron: Toward a new  $^{40}\text{Ar}/^{39}\text{Ar}$  timescale of reversals and events, *J. Geophys. Res.* 104 (1999) 679–693.
- [6] S. Cande, D.V. Kent, A new Geomagnetic Polarity Time Scale for the Late Cretaceous and Cenozoic, *J. Geophys. Res.* 97 (1992) 13917–13951.
- [7] A.P. Roberts, J.C. Lewin-Harris, Marine magnetic anomalies: evidence that ‘tiny wiggles’ represent short-period geomagnetic polarity intervals, *Earth Planet. Sci. Lett.* 183 (2000) 375–388.
- [8] L.M. Chambers, M.S. Pringle, Age and duration of activity at the Isle of Mull Tertiary igneous center, Scotland, and confirmation of the existence of subchrons during Anomaly 26r, *Earth Planet. Sci. Lett.* 193 (2001) 333–345.
- [9] R.R. Doell, A.V. Cox, The Pacific geomagnetic secular variation anomaly and the question of lateral uniformity in the lower mantle, in: E.C. Robertson (Ed.), *The Nature of the Solid Earth*, McGraw-Hill, New York, 1972, pp. 245–284.
- [10] G.A. Glatzmaier, R.S. Coe, L. Hongre, P.H. Roberts, The role of the Earth’s mantle in controlling the frequency of geomagnetic reversals, *Nature* 401 (1999) 885–890.
- [11] D. Gubbins, The distinction between geomagnetic excursions and reversals, *Geophys. J. Int.* 137 (1999) F1–F3.
- [12] K. Zhang, D. Gubbins, On convection in the Earth’s core driven by lateral temperature variations in the lower mantle, *Geophys. J. Int.* 108 (1992) 247–255.

- [13] X. Quidelleur, J. Holt, J.P. Valet, Confounding influence of magnetic fabric on sedimentary records of a field reversal, *Nature* 374 (1995) 246–249.
- [14] P. Rochette, Rationale of geomagnetic reversals versus remanence recording processes in rocks: a critical review, *Earth Planet. Sci. Lett.* 98 (1990) 33–39.
- [15] P. Roperch, N. Bonhommet, S. Levi, Paleointensity of the Earth's magnetic field during the Laschamp excursion, *Earth Planet. Sci. Lett.* 88 (1988) 209–219.
- [16] D.E. Champion, M.A. Lanphere, M.A. Kuntz, Evidence for a new geomagnetic reversal from lava flows in Idaho: Discussion of short polarity reversals in the Brunhes and Late Matuyama polarity chrons, *J. Geophys. Res.* 93 (1988) 11667–11680.
- [17] J.W. Holt, J.L. Kirschvink, F. Garnier, Geomagnetic field inclinations for the past 400 kyr from the 1-km core of the Hawaii Scientific Drilling Project, *J. Geophys. Res.* 101 (1996) 11655–11663.
- [18] P. Shane, T. Black, J. Westgate, Isothermal plateau fission-track ages for a paleomagnetic excursion in the Makaku Ignimbrite, New Zealand, and implications for the late Quaternary stratigraphy, *Geophys. Res. Lett.* 21 (1994) 1695–1698.
- [19] E. Schnepf, H. Hradetzky, Combined paleointensity and  $^{40}\text{Ar}/^{39}\text{Ar}$  age spectrum data from volcanic rocks of the West Eifel field (Germany): Evidence for an early Brunhes geomagnetic excursion, *J. Geophys. Res.* 99 (1994) 9061–9076.
- [20] X. Quidelleur, P.-Y. Gillot, J. Carlot, V. Courtillot, Link between excursions and paleointensity inferred from abnormal field directions recorded at La Palma around 600 ka, *Earth Planet. Sci. Lett.* 168 (1999) 233–242.
- [21] S. Plesner, J.R. Wilson, P.M. Holm,  $^{40}\text{Ar}/^{39}\text{Ar}$  Geochronology of Santo Antão, Cape Verde Islands, *J. Volcanol. Geotherm. Res.* 120 (2002) 103–121.
- [22] J.B. Bebiano, A geologia do Arquipélago de Cabo Verde, *Port. Serv. Geol. Commun.* 18 (1932) 276.
- [23] B.P. Dash, M.M. Ball, G.A. King, L.W. Butler, P.A. Rona, Geophysical investigation of the Cape Verde Archipelago, *J. Geophys. Res.* 100 (B7) (1995) 10013–10027.
- [24] M. McNutt, Thermal and mechanical properties of the Cape Verde Rise, *J. Geophys. Res.* B 9 (1988) 2784–2794.
- [25] J. Klerkx, P. De Paepe, The main characteristics of the magmatism of the Cape Verde Islands, *Ann. Soc. Geol. Belg.* 99 (1976) 347–357.
- [26] D.E. Hayes, P.D. Rabinowitz, Mesozoic magnetic lineations and the magnetic quiet zone off Northwest Africa, *Earth Planet. Sci. Lett.* 28 (1975) 105–115.
- [27] C.J. Stillman, H. Furnes, M.J. LeBas, A.H.F. Robertson, J. Zielonka, The geological history of Maio, Cape Verde Islands, *J. Geol. Soc. London* 139 (1982) 347–361.
- [28] D.C. Gerlach, R.A. Cliff, G.R. Davies, M. Norry, N. Hodgson, Magma sources of the Cape Verdes archipelago: Isotropic and trace element constraints, *Geochim. Cosmochim. Acta* 52 (1988) 2979–2992.
- [29] P. De Paepe, J.H. Klerkx, P. Plinke, Oceanic tholeiites on the Cape Verde Islands: Petrochemical and geochemical evidence, *Earth Planet. Sci. Lett.* 22 (1974) 347–354.
- [30] N. Watkins, A. Richardson, R.G. Mason, Palaeomagnetism of the Macaronesian Insular Region, The Cape Verde Islands, *Geophys. J. R. Astron. Soc.* 16 (1968) 119–140.
- [31] K. Storetvedt, R. Løvlie, Magnetization properties of intrusive/extrusive rocks from East Maio (Republic of Cape Verde) and their geological implications, *Geophys. J. R. Astron. Soc.* 73 (1983) 197–212.
- [32] M.C. Abranches, K.M. Storetvedt, A. Serralheiro, R. Løvlie, The palaeomagnetic record of the Santiago volcanics (Republic of Cape Verde); multiphase magnetization and age consideration, *Phys. Earth Planet. Inter.* 64 (1990) 290–302.
- [33] M.F. Knudsen, N. Abrahamsen, Magnetostratigraphy of young Pliocene volcanics at Santo Antão, Cape Verde Islands: The Escabecada and Chã de Morte Profiles, *Phys. Chem. Earth* 25 (2000) 461–467.
- [34] R. Day, M. Fuller, V.A. Schmidt, Hysteresis properties of titanomagnetites: Grain-size and compositional dependence, *Phys. Earth Planet. Inter.* 13 (1977) 260–267.
- [35] D. Dunlop, Theory and application of the Day plot ( $M_{rs}/M_s$  versus  $H_{cr}/H_c$ ). 1. Theoretical curves and tests using titanomagnetite data, *J. Geophys. Res.* 107 (2002).
- [36] J.L. Kirschvink, The least squares line and plane and the analysis of palaeomagnetic data, *Geophys. J. R. Astron. Soc.* 62 (1980) 699–718.
- [37] P.L. McFadden, M.W. McElhinny, Classification of the reversal test in palaeomagnetism, *Geophys. J. Int.* 103 (1990) 725–729.
- [38] M.W. McElhinny, P.L. McFadden, Paleosecular variation over the past 5 Myr based on a new generalized data base, *Geophys. J. Int.* 131 (1997) 240–252.
- [39] C. Laj, A. Mazaud, R. Weeks, M. Fuller, E. Herrero-Bervera, Geomagnetic reversal paths, *Nature* 351 (1991) 447.
- [40] C. Laj, A. Mazaud, R. Weeks, M. Fuller, E. Herrero-Bervera, Statistical assessment of the preferred longitudinal bands for recent geomagnetic field reversal records, *Geophys. Res. Lett.* 19 (1992) 2003–2006.
- [41] K.A. Hoffman, Long-lived transitional states of the geomagnetic field and the two dynamo families, *Nature* 354 (1991) 273–277.
- [42] K.A. Hoffman, Dipolar reversal states of the geomagnetic field and core-mantle dynamics, *Nature* 359 (1992) 789–794.
- [43] C.G. Langereis, M.J. Dekkers, G.J. de Lange, M. Paternò, P.J.M. van Santvoort, Magnetostratigraphy and astronomical calibration of the last 1.1 Myr from an eastern Mediterranean piston core and dating of short events in the Brunhes, *Geophys. J. Int.* 129 (1997) 75–94.
- [44] D. Kent, S.R. Hemming, B.D. Turrin, Laschamp Excursion at Mono Lake, *Earth Planet. Sci. Lett.* 197 (2002) 151–164.
- [45] U. Bleil, G. Gard, Chronology and correlation of Quaternary magnetostratigraphy and nannofossil biostratigraphy

- in Norwegian-Greenland Sea sediments, *Geol. Rundsch.* 78 (1989) 1173–1187.
- [46] D.K. Biswas, M. Hyodo, Y. Taniguchi, M. Kaneko, S. Katoh, H. Sato, Y. Kinugasa, K. Mizuno, Magnetostratigraphy of Plio-Pleistocene sediments in a 1700-m core from Osaka Bay, southwestern Japan, short geomagnetic events in the middle Matuyama, early Brunhes chrons, *Palaeogeogr. Palaeoclimatol. Palaeoecol.* 148 (1999) 233–248.
- [47] S. Plesner, Petrology and Geochronology of Santo Antão, Cape Verde Islands, unpublished Ph.D. Thesis, Department of Earth Sciences, Aarhus University, 2002.